Journal of Power Sources 183 (2008) 643–650

Contents lists available at ScienceDirect

Journal of Power Sources

journal homepage: www.elsevier.com/locate/jpowsour

Gas–liquid two-phase flow patterns in parallel channels for fuel cells

Lifeng Zhang[a], Hsiaotao T. Bi[a,*], David P. Wilkinson[a], Jürgen Stumper[b], Haijiang Wang[c]

[a] Department of Chemical and Biological Engineering, The University of British Columbia, Vancouver, Canada V6T 1Z3
[b] Automotive Fuel Cell Cooperation Corporation, 9000 Glenlyon Parkway, Burnaby, BC, Canada, V5J 5J8
[c] NRC Institute for Fuel Cell Innovation, Vancouver, Canada V6T 1W5

ARTICLE INFO

Article history:
Received 15 April 2008
Received in revised form 26 May 2008
Accepted 26 May 2008
Available online 8 June 2008

Keywords:
Flow hysteresis
Flow mal-distribution
Gas–liquid two-phase flow
Pressure drop
Parallel channels
PEM Fuel cell

ABSTRACT

Two-phase flow in horizontal parallel channels has been experimentally investigated under fuel cell related operating conditions. Pronounced hysteresis is observed in the pressure drop versus flow characteristic curve when starting from either flooded or dry conditions. When gas is introduced into channels initially filled with water (flooded initial condition), both gas and liquid tend to flow predominantly in one channel at low gas or liquid flow velocities. As the gas flow velocity increases, even distribution of gas and liquid flow in both channels is observed, accompanied with a sudden decrease in the pressure drop. On the other hand, even gas and liquid flow distribution between both channels is found at comparatively lower gas flow velocities when starting with dry-gas flow conditions with liquid introduced into channels filled with gas (stratified flow regime). The flow regimes of this system are visualized in plots of the pressure drop against gas and liquid flow velocities. However, this phenomenon tends to vanish at high gas and liquid flow velocities, suggesting that high gas and liquid flow velocities are required to ensure even flow distribution in parallel channels. The hysteresis points appear at the same level of the pressure drop, reflecting intrinsic characteristics of the parallel channels used in this study. These results have important implications for PEM fuel cell operational strategies. In order to avoid reactant mal-distribution in parallel flow channels in the flow field in the two-phase flow regime, fuel cells should be operated at sufficiently high gas flow velocities.

1. Introduction

The flow distribution of gas and liquid in parallel channels has received much attention due to its importance in many engineering applications. Particularly, in fuel cells, flow fields typically consist of multiple parallel mini-channels with sub-millimeter dimensions. Under typical operating conditions, especially for automotive applications, the reactant gas on the cathode invariably saturates, leading to the presence of liquid water in the flow channels [1]. Therefore, it is important to develop a better understanding of two-phase flow in mini-channels in order to ensure uniform homogeneous reactant distribution under all operating conditions. Under two-phase flow conditions, equal pressure drop does not ensure even distribution of gas and liquid in multiple channels, because different combinations of gas and liquid flow rates can yield the same pressure drop. Consequently, the resulting mal-distribution of gas and liquid can lead to flooding or drying in different regions of the active cell area. The presence of flooding and drying regions leads to current re-distribution which can significantly impact fuel cell performance and can also lead to cell instabilities characterized by erratic changes in pressure drop and cell performance [2–6]. Therefore, an improved fundamental understanding of gas and liquid flow in parallel mini-channels is required in order to design reliable flow fields for stable fuel cell operation.

In the literature, much effort has been devoted to gas and liquid distribution in engineering applications such as heat exchangers, condensers, cooling system in nuclear reactors [7–9]. In general, flow mal-distribution and flow hysteresis in parallel channels is considered to be associated with the presence of a negative slope of pressure drop against gas velocity, which happens in the transition region between bubbly flow and annular (or capillary slug) flow [7]. Similarly, such two-phase flow induced flow mal-distribution and flow hysteresis, if not properly understood and avoided in the fuel cell operation, can negatively impact cell performance through potential loss and current density shifts. There appears to be no studies on the instability-induced mal-distribution in fuel cell flow channels reported in the open literature. As a result, most existing gas flow fields including the most advanced interdigitated gas distributor have been designed based on single-phase flow principles, and they have not been able to prevent the mal-distribution of two-phase flow in gas flow channels. Recently, Maharudrayya et al.

* Corresponding author. Fax: +1 604 8226003.
E-mail addresses: xbi@chml.ubc.ca (H.T. Bi), dwilkinson@chml.ubc.ca (D.P. Wilkinson).

0378-7753/$ – see front matter © 2008 Elsevier B.V. All rights reserved.
doi:10.1016/j.jpowsour.2008.05.080

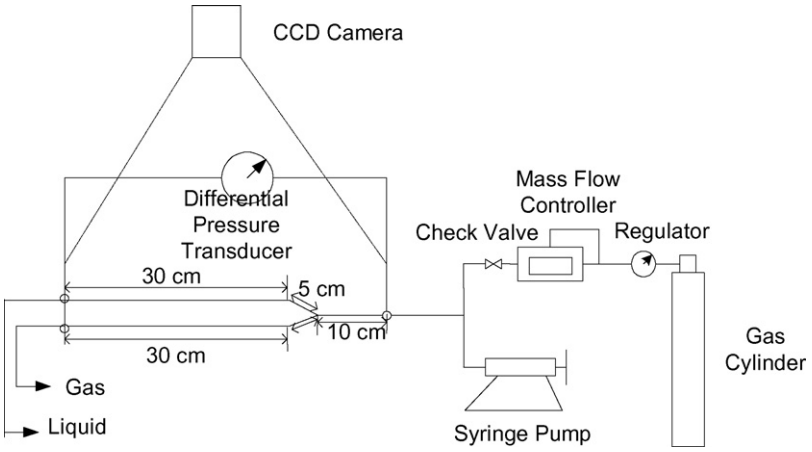

Fig. 1. Schematic of the experimental setup.

[10,11] attempted to establish a pressure drop model in the inlet and exhaust gas header to analyze flow distribution in parallel channels. However, their analysis was solely based on single-phase gas flow and the negative pressure slope characteristics in the gas–liquid mixture flow were not taken into account. Therefore, flow maldistribution and flow hysteresis cannot be properly understood employing their results.

The objective of the present work is to investigate flow maldistribution and flow hysteresis of gas and liquid two-phase flow in parallel mini-channels through visualization and pressure drop measurement at flow conditions of relevance to fuel cell operation. A proper operation zone was then identified in order to avoid flooding and drying conditions in the flow channels based on our experimental results.

2. Experimental

The experimental setup is schematically shown in Fig. 1. The experiments were conducted in Y-branched parallel square channels of 1.59 mm × 1.59 mm. The channels were fabricated in a clear acrylic plate using a conventional milling machine. The length of the straight section of the parallel channels is 300 mm, and Y-branch out leg section is 50 mm in length with the angle of the branch at 30 degrees. An introduction channel of 3.2 mm in width, 1.59 mm in depth and 100 mm long connected the Y-branch to the inlet.

Two types of channel exit design were investigated. As shown in Fig. 2, the first design consists of a vertical section of about 30 mm to direct the outflow, while the second design has a straight-out exit.

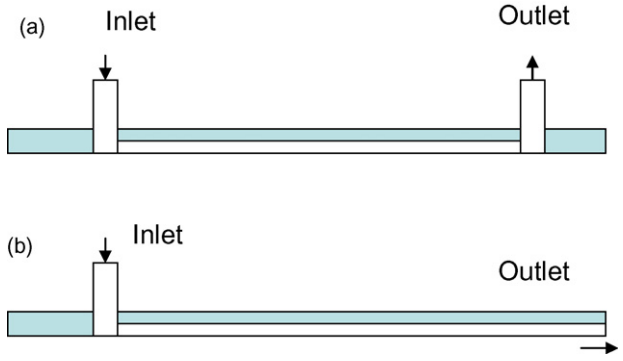

Fig. 2. Sideview of flow channels with (a) vertical exits and (b) straight-through exits.

Air was supplied through a pressurized gas cylinder and the gas flow rate was measured through a mass flow meter (AALBORG, GFM17), with a maximum flow rate of 5 SLPM. A check valve was installed in order to protect water back flow into the mass flow meter. Water was injected into the channel by a syringe pump (Cole–Parmer 74900-00) with a maximum flow capacity of 350 ml h^{-1}. The pressure drop across the test section was measured by a Micro Switch differential pressure drop transducer with a maximum pressure difference range of 2000 Pa. Visualization of the two-phase flow was conducted with a Canon CCD camera at a standard frame speed of 30 frames s^{-1}.

During the course of experiments, the gas and liquid flow rates were controlled within typical operating conditions of active PEM fuel cells, with the superficial gas velocity ranging from 0 to 10 m s^{-1} and the superficial liquid velocity from 0 to 0.03 m s^{-1}, resulting in Reynolds numbers in the ranges of 1–150 for liquid phase and 10–1000 for gas phase, respectively. Under current operating conditions, Capillary number ranges from 10^{-5} to 10^{-3}, indicating a dominant effect of surface tension versus viscous force. Those test conditions correspond to fuel cell operating conditions with equivalent current densities of 0–10 A cm^{-2} and a maximum stoichiometric ratio of 100. At a constant liquid velocity, the gas velocity was changed in two different experiments. In experiment 1, the initial flow was pure water, and the gas velocity was increased from zero to simulate initial flooding conditions. However, in experiment 2, the gas flow rate was decreased from an initial maximum gas flow rate at a given liquid flow rate, corresponding to a dry condition. For purposes of comparison, the pressure drop was also measured in a single channel of the Y-branched parallel two-channel system by blocking the flow into the other channel.

3. Results and discussion

3.1. Flow patterns

Detailed flow regime maps for gas–liquid two-phase flow in single mini-channels have been studied in detail by Triplett et al. [12] and Kawahara et al. [13], among others. In addition, typical two-phase flow regimes in cathode gas channels of active fuel cells can be found in the recent work from Zhang et al. [14]. The present work is focused on investigating flow patterns in two identical parallel channels, with emphasis on the distribution of gas and liquid flow in the two channels under conditions of relevance to fuel cell operations. Four flow distribution patterns as shown in Fig. 3 have been identified throughout the tests in this study, and

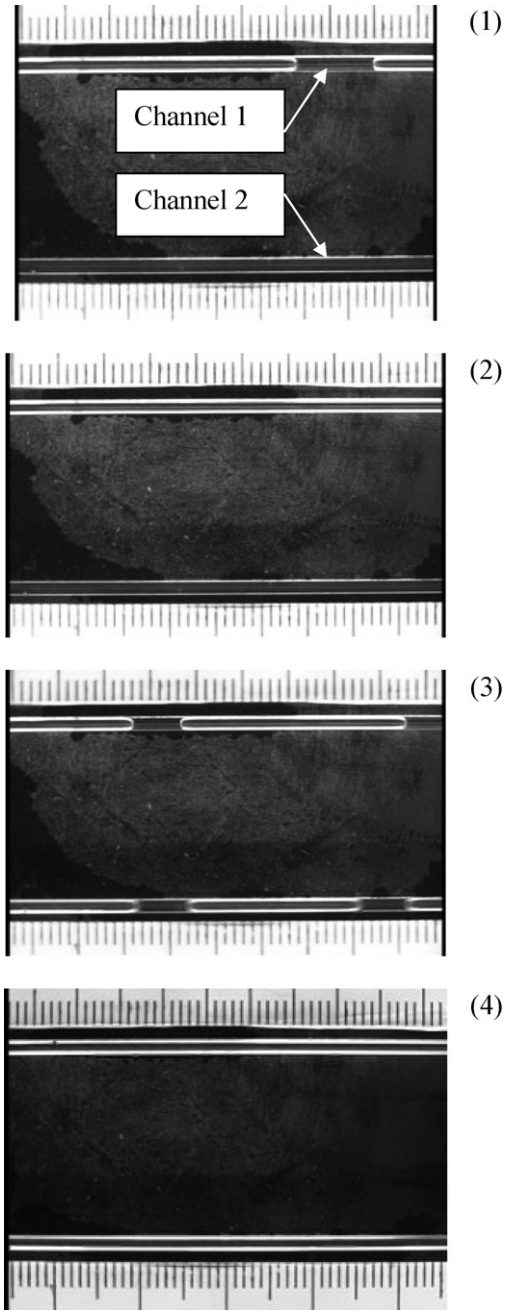

Fig. 3. Typical flow patterns for two parallel channels. Dark: liquid; light: gas. (1) Slug flow + stagnant liquid (u_L = 0.0066 m s^{-1} and u_G = 0.395 m s^{-1} @ ascending approach). (2) Stratified flow + stagnant liquid (u_L = 0.0033 m s^{-1} and u_G = 3.56 m s^{-1} @ ascending approach). (3) Slug flow in both channels (u_L = 0.0267 m s^{-1} and u_G = 0.197 m s^{-1} @ ascending approach). (4) Stratified flow in both channels (u_L = 0.0016 m s^{-1} and u_G = 6.32 m s^{-1} @ descending approach).

are used to facilitate the characterization of the flow distribution and to construct the flow distribution map in the present work. It is important to note that the flow pattern in the two channels alternated during repeated runs, confirming that the mal-distribution across the two channels is not induced by a difference or defect in the two parallel channels. However, channel heterogeneity, including either geometric heterogeneity or surface wettability variation around the flow, or both, can also lead to flow mal-distribution [15].

In flow pattern (1), there is slug flow in one channel while the other one is filled with stagnant liquid, which usually occurs at low gas velocities. As the gas velocity increases, gas slugs in one

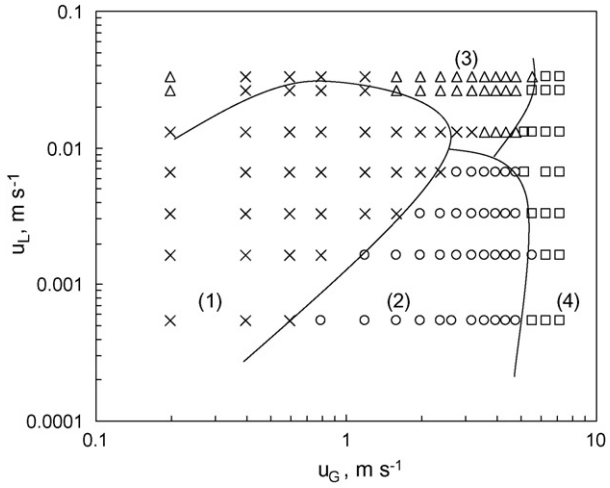

Fig. 4. Flow patterns in parallel channels as observed with increasing the gas velocity. (Ascending process) at various given liquid velocities. (1) ×: slug flow + stagnant liquid; (2) ○: stratified flow + stagnant liquid; (3) △: slug flow in both channels; (4) □: stratified flow in both channels. Solid lines define boundaries between flow patterns.

channel gave way to stratified flow, as depicted in flow pattern (2). Slug flow in two channels constitutes flow pattern (3). At relatively high gas velocities, no liquid slugs can be observed due to significant shear stress dominating over the surface tension. Therefore, stratified (annular) flow in two channels is obtained, as depicted by flow pattern (4). Based on experiments by increasing and decreasing gas flow rates, following the two test paths, at various constant liquid velocities, the flow patterns in the two parallel channels are identified and shown in Figs. 4 and 5, respectively.

As indicated in Fig. 4, when the system starts from the initial flooding conditions, uniform flow distribution into two channels cannot be reached until at very high gas velocities (regime 4). Slug flow in both channels (regime 3) occurs at medium levels of gas flow rates and high liquid flow rates. At low gas velocities, however, gas tends to go through one channel preferentially, leaving the other channel remaining filled with liquid only, as shown in regime 1 and regime 2. This observation is consistent with previous work

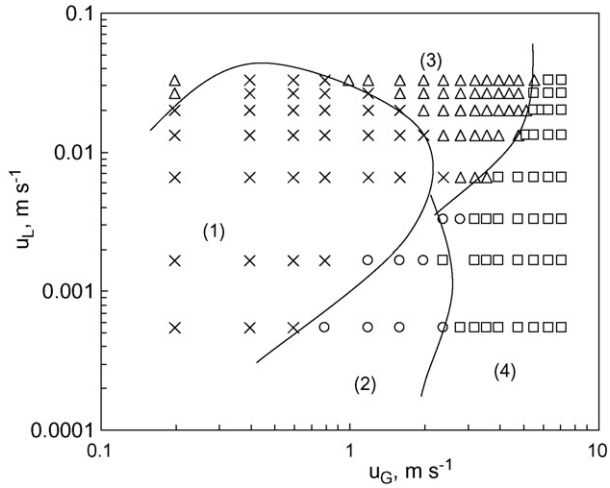

Fig. 5. Flow patterns in parallel channels as observed with decreasing the gas velocity. (Descending process) at various given liquid flow rates. (1) ×: slug flow + stagnant liquid; (2) ○: stratified flow + stagnant liquid; (3) △: slug flow in both channels; (4) □: stratified flow in both channels. Solid lines define boundaries between flow patterns.

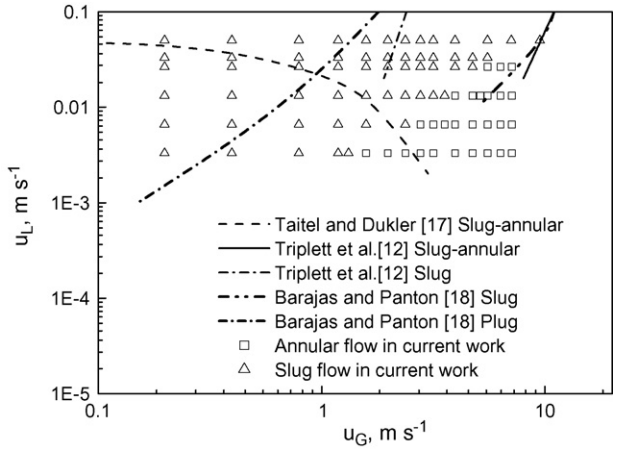

Fig. 6. Comparison of flow regimes in a single channel system with a vertical exit.

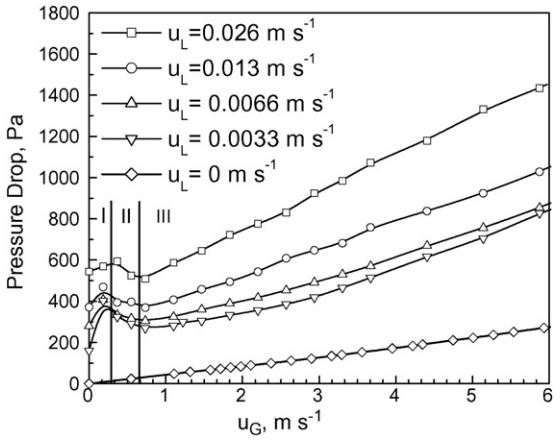

Fig. 7. Pressure drop characteristics in a single flow channel system with a vertical exit.

that at low gas velocities, both gas and liquid tend to flow in one channel of parallel channel systems [8,16]. Fig. 5 shows the flow pattern distribution identified with decreasing the gas velocity from a stratified flow condition. Compared to the flow patterns obtained in the gas ascending process, there is a wider region for slug flow and stratified flow in both channels (regime 3 and regime 4) in the gas descending process. In addition, the region of stratified flow and stagnant liquid (regime 2) appears to be much narrower in the gas flow descending process.

Due to the novelty of the flow pattern diagrams developed in the present study for two parallel flow channels under two-phase flow conditions, no literature data have been reported for comparison with the current flow pattern diagram. Instead, the flow regime in a single channel measured when one of the two parallel channels was completely blocked was obtained and used to compare with the literature. Since many studies of two-phase flow in mini-channels have been devoted to relatively high liquid velocities beyond those typically encountered in fuel cell operations, only those with similar liquid flow rate ranges were selected and compared with our results. It is seen in Fig. 6 that the flow regime transition predicted from the model by Taitel and Dukler [17] shows a large deviation from the experimental results, indicating that the flow regime maps developed from their model are not intended for very small channels where surface tension becomes an important factor. Compared to flow patterns for the 1.45 mm circular mini-channel from Triplett et al. [12], there is a relatively good agreement in the slug and annular flow regimes while in the present work there is not a noticeable transition regime observed. The flow patterns in a 1.6-mm circular tube from Barajas and Panton [18] shows relatively good agreement with our data in the slug flow regime, while there is not a plug flow regime observed in the present setup, presumably due to the corner effect of the square cross-section of our test channel.

In parallel channels, the difference of the flow patterns obtained in the gas ascending and descending paths indicates that multiple steady states can exist at the same superficial gas and liquid velocities. The tendency of gas and liquid flow in one or two channels is not only determined by the operating parameters such as gas velocities and liquid velocities but also influenced by the operational procedures adopted, i.e., ascending or descending change in gas flow rates. Similar hysteresis phenomena are commonly encountered in non-linear systems such as non-isothermal reactors when heat generation and heat removal are involved [19]. Also, when the flow pattern switched from non-uniform flow to uniform flow distribution or between different flow regimes in the two parallel channels, the pressure drop versus flow characteristics shows a distinct change. This will be discussed in detail in the following section.

3.2. Pressure drop

3.2.1. Pressure drop in a single channel

The pressure drop in a single flow channel was measured by blocking one of the two parallel channels, allowing the gas–liquid mixture to flow through the unblocked channel only. The dependence of the pressure drop on gas flow rate and liquid flow rate in a single flow channel is shown in Fig. 7. For purposes of comparison, the pressure drop in pure gas flow is also given in this figure. In general, three (with the transition region of negative flow resistance slope as an additional region) regions can be defined according to the relationship between the pressure drop and gas flow rates under two-phase flow conditions. In region I, the pressure drop at a given liquid flow rate generally increases with increasing gas flow rate and approaches a maximum, in region II it decreases with further increase in the gas flow rate. After reaching a minimum value, the pressure drop increases again with an increase in the gas flow rate, with the region defined as region III in Fig. 7. The trend of the pressure drop in region II is attributed to flow regime changes, as reported by Ozawa et al. [7]. Although similar experimental observations on this negative flow resistance slope have been reported in the literature by some researchers [7,20], there has been no single equation or model, which can predict such a phenomenon. Based on the observations in this study and the literature, it is speculated that this negative flow resistance slope in region II is closely linked to the observed flow mal-distribution of the gas and liquid mixture in parallel flow channels. In the annular flow regime of Fig. 6 and the flow pattern 2 region of Figs. 4 and 5, the dependence of the pressure drop on the gas flow rate is consistent with what is expected from most existing models where the pressure drop increases monotonically with increasing the gas velocities. However, the transition region II in Fig. 6 in a single channel system and flow pattern 2 region of Figs. 4 and 5 in parallel channels seem to correspond to each other.

3.2.2. Pressure drop in parallel channels

A typical example of the pressure drop against gas flow rate in Y-branch parallel channels is shown in Fig. 8. The solid line represents the pressure drop data obtained following the gas ascending process whereas the dotted line represents the data from the gas descending process. As the gas velocity increases, there is a slight increase in the pressure drop with an increase in the gas flow rate,

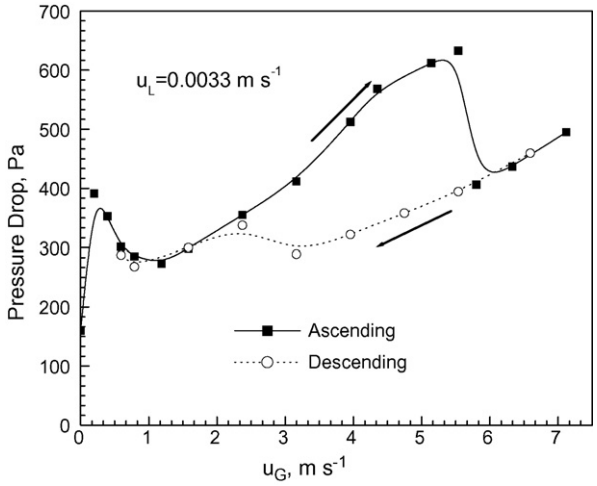

Fig. 8. Pressure drop characteristics in parallel channels with a vertical exit ($u_L = 0.0033\ m\ s^{-1}$).

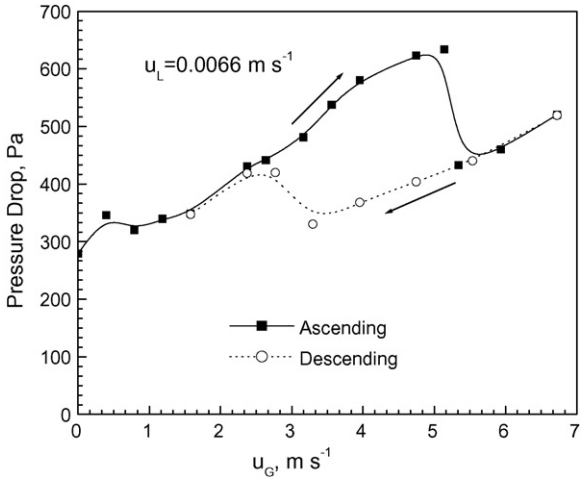

Fig. 9. Pressure drop characteristics in parallel channels with a vertical exit ($u_L = 0.0066\ m\ s^{-1}$).

followed by a decrease to reach a minimum before increasing again. This is similar to what happens in a single channel system as shown in Fig. 7. When the gas velocity is increased to about 5.5 m s^{-1}, a critical point is reached beyond which a sudden drop in pressure drop occurs with a further increase in gas velocity, as shown in Fig. 8. Thereafter, the pressure drop resumes its trend to increase again with further increase in the gas velocity. Similar to Fig. 7, the observed regions of negative flow resistance slope indicate a flow regime transition. More specifically, the transitions between flow patterns 1 and 2 as well as 2 and 4 (see Fig. 4), which occur at around 1 m s^{-1} and 5 m s^{-1}, respectively.

The flow pattern transforms from pattern (2) with stratified flow in one channel and stagnant liquid in the other channel to pattern (4) with stratified flow in both channels at a gas velocity of about 5.5 m s^{-1}, which corresponds to the sudden decrease in the pressure drop in Fig. 8. When the gas velocity decreases from a high gas flow rate with stratified flow in both channels, the pressure drop decreases following a substantially different trajectory/path (dotted line). However, the two pressure drop trajectories merge together when the gas velocity decreases to a certain value with a superficial gas velocity of about 2 m s^{-1}. Similar to the previous analysis, it is found that such a pressure drop versus gas velocity hysteresis phenomenon corresponds to a flow pattern transition. In the hysteresis region, the flow pattern is in the uniform stratified flow regime in both channels in the flow descending process as shown in Fig. 5, but the flow is in stratified flow in one channel while the other channel is in stagnant liquid flow in the flow ascending process according to Fig. 4. It is also interesting to be noted that consistent flow patterns are observed in the single straight introduction channel before the gas and liquid flows split into the Y-branched channels in both the flow ascending and descending processes.

The same trend is also observed at a higher superficial liquid velocity of 0.0066 m s^{-1} as shown in Fig. 9. However, the flow hysteresis occurs at a superficial gas velocity range of 2.5–5.5 m s^{-1}, indicating that there is a smaller hysteresis zone at higher liquid flow rates as further evidenced by Figs. 10 and 11.

Unique to this system, the peak pressure drop at the critical point appears to remain at a constant value of approximately 630 Pa as shown in Figs. 8–11 for the parallel channels with an a-type exit. The value of this peak pressure drop and the nature of the hysteresis region likely reflect some intrinsic characteristics of the current parallel channel design such as the channel configuration, channel surface roughness, channel surface hydrophobicity, and inlet and

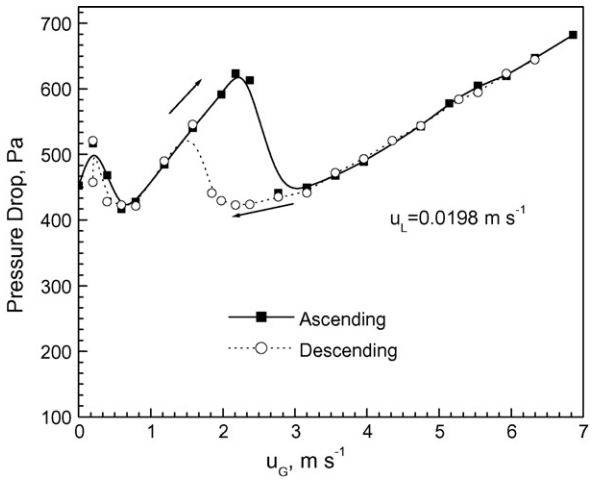

Fig. 10. Pressure drop characteristics in parallel channels with a vertical exit ($u_L = 0.0198\ m\ s^{-1}$).

outlet configuration, presence of gas shorting between channels, etc., which requires further investigation in the future.

In order to test this hypothesis, we considered that the orientation of the outlet may also play a role on the flow hysteresis

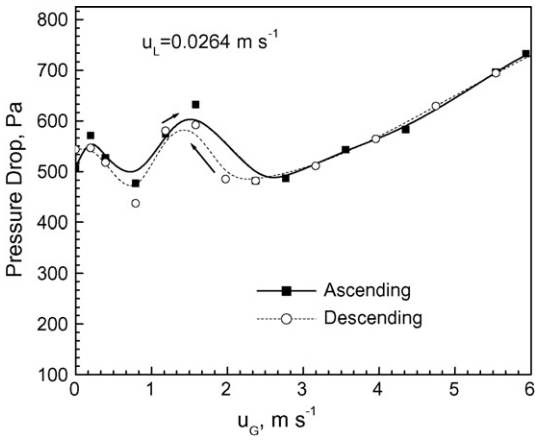

Fig. 11. Pressure drop characteristics in parallel channels with a vertical exit ($u_L = 0.0264\ m\ s^{-1}$).

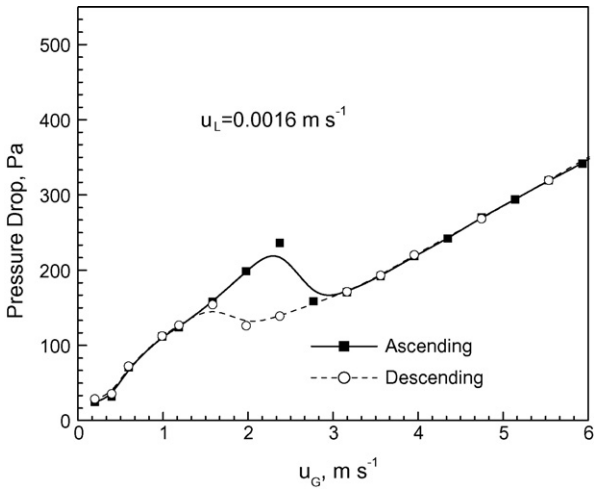

Fig. 12. Pressure drop in parallel channels with a straight-through exit ($u_L = 0.0016\,m\,s^{-1}$).

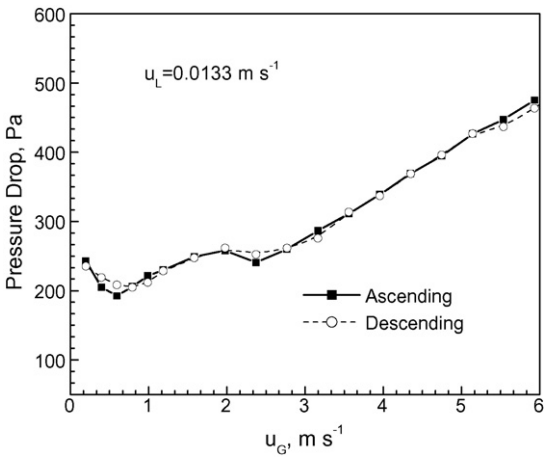

Fig. 14. Pressure drop in parallel channels with a straight-through exit ($u_L = 0.0133\,m\,s^{-1}$).

phenomenon. Therefore, experiments were performed on a modified setup with two straight-through channels, i.e., the b-type exit design as shown in Fig. 2. Typical plots of the pressure drop versus gas flow rates are shown in Figs. 12–14 for the straight-through channel outlet configuration. The flow hysteresis phenomenon occurs at two low liquid velocities of 0.0016 m s^{-1} and 0.0033 m s^{-1}, as shown in Figs. 12 and 13, respectively. In addition, for purposes of comparison, the pressure drop behavior at two different outlet configurations with the liquid velocities being the same are compared in Fig. 13. Compared to Figs. 8–10 obtained with the vertical outlet configuration, i.e., the a-type exit configuration, the hysteresis regions are narrower and the peak pressure drop is lower for the channels with a straight-through outlet. However, the flow hysteresis vanished at a liquid velocity of 0.0133 m s^{-1} for the straight-through flow channel outlet, as shown in Fig. 14. The presence of the sudden change in pressure drop in Figs. 12–14 indicates the existence of a flow pattern change from non-uniform distribution to uniform distribution. The critical peak pressure drop for this configuration remains at a constant value of approximately 240 Pa.

From the comparison of the two outlet configurations, it seems that the straight-through channel is a better design since it has a smaller hysteresis region and the uniform distribution occurs at lower gas flow rates. This appears to be consistent with the findings from inclined parallel pipes in the previous work of Tshuva et al. [21] in parallel pipes of 2.4 cm in diameter and 3 m in length, who reported that the region of flow mal-distribution increased as the inclination angle increased. Therefore, it is expected that the flow hysteresis region will be broader in vertical channels than horizontal channels due to the influence of the gravitational hydrostatic pressure drop induced. For that matter, any additional pressure drop at the outlet of a fuel cell parallel flow channels would be expected to influence the flow hysteresis region and flow maldistribution, and should be taken into account in the fuel cell design.

3.3. Pressure fluctuations

Pressure drop fluctuations can also provide important information about the flow system. They arise from many factors such as density fluctuations, flow rate fluctuations, pressure waves originating from other sources and transducer noises, etc. In the present work, standard deviations are used as a measure of the pressure fluctuations. Fig. 15 shows the standard deviation of pressure drop fluctuations for a single flow channel. The fluctuation is seen to increase with increasing gas flow rate at a given liquid velocity before reaching a maximum and then decreases with further

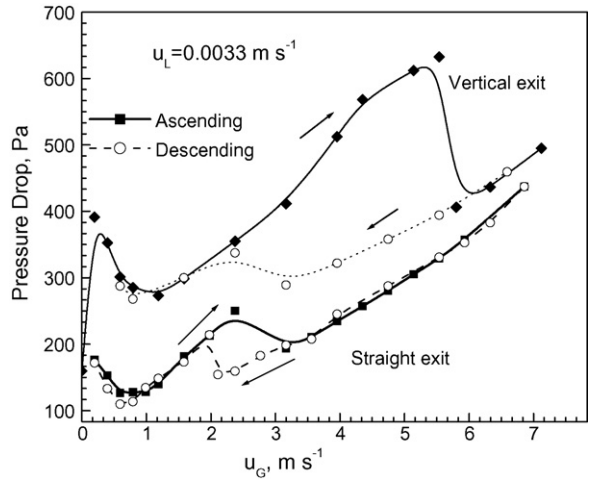

Fig. 13. Pressure drop in parallel channels with a straight-through exit ($u_L = 0.0033\,m\,s^{-1}$).

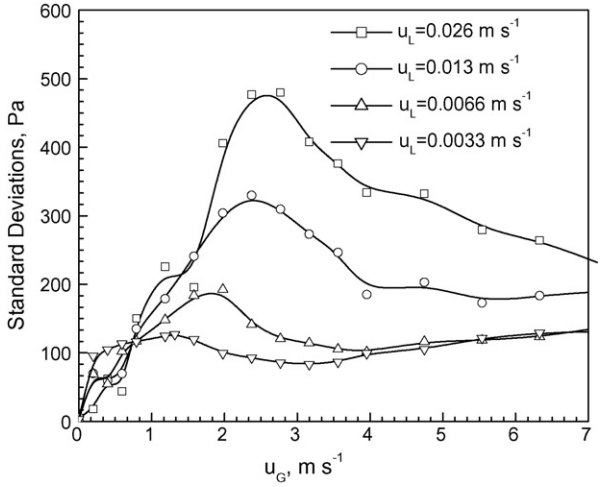

Fig. 15. Standard deviations of the pressure drop fluctuations in the single channel system with a vertical exit.

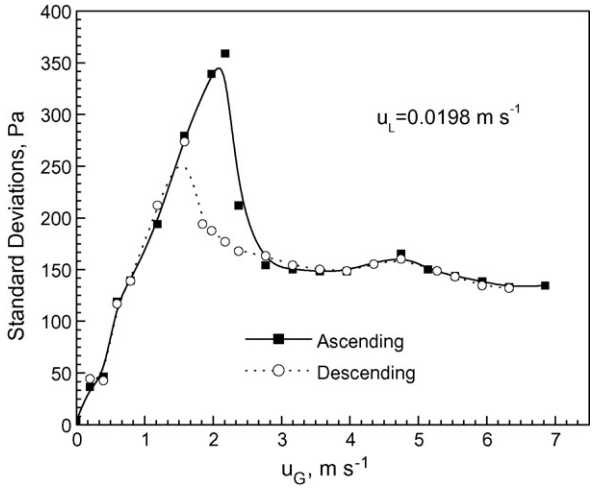

Fig. 16. Standard deviations of the pressure drop in the parallel channel system with a vertical exit.

increase in the gas flow rate. The maximum pressure fluctuation point appears to correspond to the transition from slug flow to stratified/annular flow patterns in the flow channel.

Fig. 16 shows the standard deviation of pressure drop fluctuations corresponding to the gas flow ascending and descending processes at a constant liquid flow rate for the parallel channel system. It is seen in this figure that the same pressure fluctuations are obtained from both the ascending and descending processes in the high gas flow and low gas flow regions. In the middle region where flow hysteresis was identified in Fig. 10, the pressure fluctuation in the flow ascending process is generally higher than the flow descending process, again indicating the different flow pattern and flow distributions in the parallel channels in the ascending and descending processes.

Similar to the averaged pressure drop, pressure fluctuations in the parallel channel system also exhibit hysteresis behavior and a sudden drop in fluctuations occurs at a gas velocity of about 2 m s^{-1} where even distribution of two-phase flow occurs. Less pressure drop fluctuations in the stratified flow regime imply that in order to obtain stable fuel cell operations, liquid water in channels is preferentially to be controlled at the stratified/annular flow. Therefore, high stoichiometry airflow is required as indicated in the previous work from Zhang et al. [14].

3.4. Implications for fuel cell stack operations

Based on the current experimental observations, it is seen that flow mal-distribution occurs in 1.59 mm × 1.59 mm parallel flow channels mainly at intermediate gas velocities 0.5–5 m s^{-1}. Furthermore, operational hysteresis and the pressure drop fluctuations tend to be lower at higher liquid velocities. Once the mal-distribution occurs, one channel might be blocked by water slugs, resulting in the loss of active areas, and the gas flow rate needs to be increased beyond a certain value to transform both channels to stratified flow. Furthermore, the flow distribution tends to be more uniform across parallel flow channels following the gas flow descending process, and less uniform in the gas flow ascending process. In the dynamic operation of a PEMFC, similar hysteresis phenomena were reported in current and voltage polarization curves obtained by sweeping fuel cells from high current densities to low densities and then in the reverse direction [22,23]. Under high current density operation flooding can be prevented by using high initial gas flows. In contrast, low reactant stoichiometry under low current density operations, for example during start-up, can lead to channel blocking and corresponding reactant mal-distribution. Therefore, the implication of the present work for the operation of a PEMFC is that the gas velocity in the flow channel needs to be maintained at sufficiently high values to avoid flow mal-distribution across the flow channels. Once the flow channels are flooded, the flow system can be purged by increasing the gas flow rate to remove water and then reducing the gas flow rate back to the normal gas flow rate, i.e., descending process. Since the flow distribution across channels tends to be more uniform at high liquid flow rates, allowing more water collected into the flow channels may lead to improvement of gas flow distribution across flow channels. However, the flooded operating condition at high water flow rate may inhibit the transport of reactant gases into and through the gas diffusion layers in the fuel cell, leading to loss of performance. In addition, the presence of water slugs will lead to high pressure drop and current fluctuations. In the present work it was shown that the outlet configuration of the parallel channel flow field has a significant effect on the flow mal-distribution and hysteresis with a lower outlet pressure drop, leading to an improvement. This highlights the importance of looking at other intrinsic characteristics of the parallel channel and fuel cell design. This will be the subject of further investigation in the future. Finally, it appears that the present experimental procedure, i.e., monitoring the pressure drop and pressure drop fluctuations in the gas flow ascending and descending processes, can be potentially used as a diagnostic tool for examining flow mal-distribution of existing fuel cell flow-field designs under active fuel cell operating conditions.

4. Conclusions

Flow patterns and pressure drop characteristics of gas–liquid two-phase flow in a Y-branched parallel channel system have been investigated. Four distinctly different flow patterns have been observed, denoted in the following by the respective flow pattern in each of the two channels: (1) slug flow + stagnant liquid, (2) stratified flow + stagnant liquid, (3) slug flow in both channels and (4) stratified flow in both channels. At low gas velocities, both gas and liquid tend to flow in one channel (flow patterns 1, 2), resulting in flow mal-distribution. For all the investigated liquid flow rates, even flow distribution of gas and liquid could always be achieved at sufficiently high gas- and/or liquid velocities. Typically, a sudden shift in the pressure drop versus gas flow characteristic is observed when the two-phase flow regime changes between any of the flow regimes mentioned above. Furthermore, a pronounced hysteresis in the pressure drop versus gas flow characteristic is observed in these flow-regime transition regions between the gas flow ascending and descending test procedures.

Practical fuel cells often have multiple parallel channels and the results highlight the importance of maintaining sufficient gas flow, particularly under low power conditions or during start-up in order to avoid reactant mal-distribution over the active cell area. On the other hand, the results also indicate that intrinsic characteristics of the channel and fuel cell geometry such as outlet configuration can significantly impact flow regimes, flow hysteresis and pressure drop thus providing a path for the optimization of flow distribution through suitable cell and flow-field design.

Acknowledgement

The authors are grateful for a strategic grant from the Natural Sciences and Engineering Research Council of Canada (NSERC) to support this work.

References

[1] J. Stumper, C. Stone, J. Power Sources 176 (2008) 468–476.
[2] K. Tüber, D. Pócza, C. Hebling, J. Power Sources 124 (2003) 403–414.
[3] F. Barbir, H. Gorgun, X. Wang, J. Power Sources 141 (2005) 96–101.
[4] K. Jiao, B. Zhou, P. Quan, J. Power Sources 154 (2006) 124–137.
[5] X. Liu, H. Guo, F. Ye, C.F. Ma, Electrochim. Acta 52 (2007) 3607–3614.
[6] P. Quan, M. Lai, J. Power Sources 164 (2007) 222–237.
[7] M. Ozawa, K. Akagawa, T. Sakaguchi, Int. J. Multiphase Flow 15 (1989) 639–657.
[8] G. Hetsroni, A. Mosyak, Z. Segal, E. Pogrebnyak, Int. J. Multiphase Flow 29 (2003) 341–360.
[9] U. Minzer, D. Barnea, Y. Taitel, Chem. Eng. Sci. 61 (2006), 7429-7259.
[10] S. Maharudrayya, S. Jayanti, A.P. Deshpande, J. Power Sources 144 (2005) 94–106.
[11] S. Maharudrayya, S. Jayanti, A.P. Deshpande, J. Power Sources 157 (2006) 358–367.
[12] A. Triplett, S.M. Ghiaasiaan, S.I. Adbel-Khalik, D.L. Sadowski, Int. J. Multiphase Flow 25 (1999) 377–394.
[13] A. Kawahara, P.M.Y. Chung, M. Kawaji, Int. J. Multiphase Flow 28 (2002) 1411–1435.
[14] F.Y. Zhang, X.G. Wang, C.Y. Wang, J. Electrochem. Soc. 153 (2006) A225–A232.
[15] Y. Wang, S. Basu, C.Y. Wang, J. Power Sources 179 (2008) 603–617.
[16] L. Pustylink, D. Barnea, Y. Taitel, AIChE. J. 52 (2006) 345–3352.
[17] Y. Taitel, A.E. Dukler, AIChE. J. 22 (1976) 47–55.
[18] A.M. Barajas, R.L. Panton, Int. J. Multiphase Flow 19 (1993) 337–346.
[19] H.S. Fogler, Elements of Chemical Reaction Engineering, Fourth ed., Prentice Hall, New York, 2004, pp. 533–546.
[20] T. Sawai, M. Kaji, T. Kasugai, H. Nakashima, T. Mori, Exp. Therm. Fluid Sci. 28 (2004) 597–606.
[21] M. Tshuva, D. Barnea, Y. Taitel, Int. J. Multiphase Flow 25 (1999) 1491–1503.
[22] H.M. Yu, C. Ziegler, J. Electrochem. Soc. 153 (2006) A570–A575.
[23] F. Weng, B. Jou, A. Su, S.H. Chan, P. Chi, J. Power Sources 171 (2007) 179–185.